MATERIALS
SCIENCE &
ENGINEERING
C

CrossMark

Silver deposition on polypyrrole films electrosynthesised onto Nitinol alloy. Corrosion protection and antibacterial activity

M. Saugo [a], D.O. Flamini [a], L.I. Brugnoni [b], S.B. Saidman [a,*]

[a] Instituto de Ingeniería Electroquímica y Corrosión (INIEC), Departamento de Ingeniería Química, Universidad Nacional del Sur, Av. Alem 1253, 8000 Bahía Blanca, Argentina
[b] Planta Piloto de Ingeniería Química, Universidad Nacional del Sur, CONICET, Camino La Carrindanga Km 7, 8000 Bahía Blanca, Argentina

ABSTRACT

The electrosynthesis of polypyrrole films onto Nitinol from sodium salicylate solutions of different concentrations is reported. The morphology and corrosion protection properties of the resulting coatings were examined and they both depend on the sodium salicylate concentration. The immobilisation of silver species in PPy films constituted by hollow rectangular microtubes was studied as a function of the polymer oxidation degree. The highest amount of silver was deposited when the coated electrode was prepolarised at −1.00 V (SCE) before silver deposition, suggesting an increase in the amount of non-oxidised segments in the polymer. Finally, the antibacterial activity of the coating against the Gram positive *Staphylococcus aureus* and *Staphylococcus epidermidis* bacteria was evaluated. Both strains resulted sensitive to the modified coatings, obtaining a slightly better result against *S. aureus*.

© 2015 Elsevier B.V. All rights reserved.

1. Introduction

Nitinol (NiTi) is an equiatomic Ni and Ti alloy which has been thoroughly studied for biomedical applications due to its shape-memory, superelasticity and biocompatibility. The most important applications are bone implants [1] and cardiovascular and urological stents [2,3]. Ni-containing alloys are known to be allergenic and carcinogenic [4] as a consequence of the release of Ni^{2+} ions into the human body, which is the most important concern when this type of materials are used. If the implants are not protected in some way, the patient may develop restenosis after a few years [5].

Covering the surface of a biomaterial with a conducting polymer is a widely investigated subject. Polypyrrole (PPy) is thought to be one of the most suitable owing to its biocompatibility [6] and the good protection it provides to different substrates, including NiTi, when it is doped with several anions and corrosion inhibitors [7–11]. In addition, PPy can be prepared electrochemically in a very fast and simple way.

Conducting polymers and silver can be combined to form a composite [12] with an enhanced conductivity and a wide range of potential applications in areas such as: antibacterial activity [13], electrocatalysis [14] and sensors [15], among others. The ability of PPy to reduce silver ions to metallic silver has been experimentally proved many times

[16–18] and several assumptions about the silver deposition mechanism have been made [19,20].

As was shown in a previous work, the electrosynthesis of hollow rectangular microtubes of PPy can be performed in neutral or alkaline solutions of salicylate (Sa) [21]. It was postulated that as a result of a local pH decrease during polymerisation, salicylic acid crystallises on the surface of the electrode and then the polymer is deposited on the external surface of these crystals [22]. Silver ions are known to form a complex with salicylate through an interaction with the carboxylate group [23,24]. It was also postulated that the presence of salicylate in the PPy matrix increases the concentration of silver ions at the polymer surface and that metallic silver can be deposited as a result of a redox reaction between the non-oxidised segments of the polymer and the silver ions [18]. In the present work, the effects of different electrode pretreatments will be analysed in an attempt to get a deeper insight into the deposition process. This study will also bring information about the optimum conditions for silver deposition.

Microorganisms that naturally live on human skin or on objects in the environment can easily infect an implant or the place of its installation during surgical intervention in spite of taking great measures of caution [25,26]. The use of antibiotics in the implants or oral administration before surgery does not provide sufficient protection; in fact, the wrong antibiotic or low doses of relevant antibiotics can create resistant strains of bacteria that are difficult to treat [27–29]. The doping of synthetic materials with metal ions such as Ag^+, Cu^{2+} and Zn^{2+} is appropriate because they exhibit antimicrobial activity at the site of the implantation and they are not cytotoxic at low concentrations.

Staphylococcus aureus and *Staphylococcus epidermidis* are the strains most frequently isolated from nosocomial infections related to orthopaedic implants and the prevalence of antibiotic-resistance in implant-associated infections is an increasing concern [30,31].

The aim of this research work is to perform the electrosynthesis of PPy films on NiTi from salicylate solutions. The effects of different treatments applied to the modified electrodes on the corrosion protection performance of the coatings and on the capacity of the films to incorporate, and afterwards to liberate, silver species are evaluated. Another objective is to test the antibacterial capacity of the samples against the Gram positive bacteria *S. aureus* and *S. epidermidis*, considering that these bacteria are the most common pathogens that cause infections when NiTi alloy implants are employed.

2. Material and methods

2.1. Film preparation

2.1.1. Polypyrrole films

The working electrodes consist of NiTi rods (chemical composition (wt.%): 55.8 Ni, 0.05 O, 0.02 C and Ti balance) embedded in a Teflon holder, with an exposed area of 0.0962 cm^2. Before each experiment, the exposed surfaces were abraded with SiC papers down to 1200 grit finish, then degreased with acetone and finally washed with triply distilled water. Following this pretreatment, the electrodes were immediately transferred to an electrochemical cell for synthesis of PPy. The counter electrode was a large Pt sheet and a saturated calomel electrode (SCE) was used as a reference electrode. All the potential values in this work are referred to SCE. A Metrohm cell of 20 cm^3 was employed for electrochemical experiments. PPy films were electrosynthesised on bare NiTi alloy using solutions containing 0.25 M Py and different concentrations of sodium salicylate (NaSa): 0.1 and 0.5 M. Solutions were purified with a saturated atmosphere of nitrogen gas at 25 °C. All chemicals were reagent grade and solutions were prepared using triply distilled water. Pyrrole (Py, Sigma-Aldrich) was freshly distilled under reduced pressure before use. Electrosynthesis of PPy films on bare NiTi electrodes was carried out using a potentiostatic technique. All the electrochemical experiments were performed utilising a potentiostat–galvanostat PAR Model 273A.

2.1.2. Silver deposition

The NiTi samples covered with PPy formed in a 0.50 M salicylate solution were prepolarised at different potentials. Afterwards, the deposition of silver was performed by immersing the coated electrodes in a 0.05 M of AgNO$_3$ solution during a certain period of time under OCP in dark conditions. Then, the estimation of silver content was carried out by an anodic stripping voltammetry with a scan rate of 0.001 V s^{-1}.

2.2. Film characterization

2.2.1. Evaluation of the corrosion performance

The corrosion performance of the coatings before and after silver deposition was evaluated. Open circuit potential (OCP) variation with time, linear polarisation and potentiostatic measurements were conducted in 0.15 M of NaCl solution, which is frequently used to simulate the biological environment. All experiments were performed utilising a potentiostat–galvanostat PAR Model 273A.

2.2.2. SEM and EDX microscopy measurements

A scanning electron microscopy (SEM), JEOL 35 CF and X-ray energy dispersive system (EDX), EDAX DX-4, were used to examine the characteristics of the electrode surface.

2.2.3. Metal concentration in chloride solution

Ni and Ti released concentrations in chloride solution from bare NiTi and PPy-coated NiTi samples were determined using inductively coupled plasma atomic emission spectrometry (ICP-AES) Shimadzu-ICPE 9000.

2.2.4. Adhesion of the films

The electrosynthesis of PPy for these measurements was performed with the procedure described in Section 2.1.1, but in this case a NiTi sheet of 1 cm^2 area was employed. The adhesion of the coatings to the NiTi surface was tested using a Scotch Magic™ double coated Tape 810 (3 M) and a Mecmesin basic force gauge (BFG 50N). The NiTi/PPy sample was fixed on a plane surface, with the coated surface facing up. One side of the double coated tape was adhered to an accessory of the dynamometer apparatus, which consisted of an arm ended in a steel circular plate. The plate was pressed downwards until the double coated tape made contact with the NiTi/PPy surface. Then, it was removed slowly in the opposite direction and the necessary force to peel-off the film was registered in the dynamometer.

2.2.5. Antibacterial properties

The antimicrobial activity of the samples was investigated and compared against a reference strain of *S. aureus* (ATCC 25923) and a clinical specimen of *S. epidermidis*. The inoculums of both microorganisms were prepared from fresh overnight broth cultures (Tripton soy broth, TSB, Difco, Detroit, MI, USA) that were incubated at 37 °C. The resulting broth cultures were used for antimicrobial susceptibility test.

The antimicrobial effectiveness of the PPy films was tested according to the model of antibiogram execution by Kirby–Bauer [32]. Also, a resistance profile for a panel of antibiotics was determined for each strain using the Kirby–Bauer test.

In a clinical setting, the Kirby–Bauer test (or disk diffusion test) would be strictly standardized (culture medium, bacterial inoculum, time and temperature of incubation) to ensure consistent and accurate results. For quality assurance purposes, one of the recommended organisms is *S. aureus* ATCC 25923 (Biosafety level 2) as the zone of inhibition for this organism is known for standard antibiotics used in staphylococcal-related infections.

The agar diffusion test was performed at Muller–Hinton agar (Britania Laboratories S.A., Argentina). For each tested microbial species, an inoculum was prepared in liquid medium, corresponding to a turbidity of 0.5 ($\approx 10^6$ Colony Forming Units, CFU ml^{-1}) on the McFarland standard.

The diffusion technique was carried out by pouring agar into Petri dishes to form 4 mm thick layers and adding dense inoculum of the tested microorganisms in order to obtain semiconfluent growth. Petri plates were left for 10 min to dry in the air and after that, samples of NiTi covered with PPy and silver were distributed, using bare NiTi and NiTi covered only with PPy as control samples. For testing sensitivity or resistance of *S. aureus* ATCC 25923 and *S. epidermidis* to standard antibiotics used in staphylococcal-related infections, impregnated discs were placed on the inoculated agar. The antibiotics (Britania Laboratories S.A., Argentina) used were: cefotaxime (30 μg), clindamycin (2 μg), erythromycin (15 μg), nitrofurantoin (300 μg), ciprofloxacin (5 μg), trimethoprim-sulfamethoxazole (25 μg), penicillin G (10 IU/mL), cephalothin (30 μg), tetracycline (30 μg), cefuroxime (30 μg), vancomycin (30 μg), chloramphenicol (30 μg), gentamicin (10 μg) and ampicillin (10 μg).

The incubation was made at 37 °C. The plates were read after 24 h for the identification of the presence or absence of zones of inhibition. When zones of inhibition were present, their diameter was measured using a sliding calliper up to 1 mm resolution.

For antibiotics, the inhibition zone diameters were interpreted as resistant (R) or sensitive (S), according to the CLSI (Clinical and Laboratory Standards Institute) recommendations for Gram positive bacteria [33].

All assays were performed in duplicate and were replicated independently on two separate trials.

2.3. Statistical analysis

Every experiment where quantitative values were obtained was performed three times to ensure reproducibility and they will be expressed as the mean value with the standard deviation given in parentheses. Whenever applicable, comparison of the experimental data was made using one-way analysis of variance (ANOVA). Statistical significance was set at $p < 0.05$. Then, the post hoc Fisher least significant difference (LSD) test was used to compare populations taken in pairs.

3. Results and discussion

3.1. Electrochemical synthesis of PPy films

The electrosynthesis of PPy onto NiTi electrodes was performed potentiostatically at 0.80 V (SCE) for 600 s, in two different NaSa solutions containing the monomer (0.25 M Py). As was found for the films formed on 316L Stainless Steel, the concentration of salicylate has a great influence in the morphology of the PPy coatings [18]. When a low concentration was used (0.10 M) the typical globular PPy morphology was observed (Fig. 1a). On the other hand, when a solution of 0.50 M of Sa was used, the morphology of the polymer was characterised by the formation of hollow rectangular microtubes (Fig. 1b). For simplification these films will be called $PPy_{0.1}$ and $PPy_{0.5}$, respectively. Both films, $PPy_{0.1}$ and $PPy_{0.5}$, exhibited a very good adherence to the NiTi substrate and they could only be removed by mechanical polishing. In order to evaluate the adhesion of the coatings, the necessary force to peel-off the films was measured. The mean adherence force obtained for NiTi/$PPy_{0.1}$ and NiTi/$PPy_{0.5}$ were 26.00 (0.46) and 28.00 (0.26) N, respectively. The measured values are larger than the ones obtained in a previous work for PPy doped with nitrate and citrate or nitrate and molybdate [11]. To perform the statistical analysis, all these measures were used: the ones obtained for NiTi/$PPy_{0.1}$ and NiTi/$PPy_{0.5}$ and the ones obtained in the mentioned paper. The values of F and p obtained with ANOVA were 1054.03 and 0.0001 respectively. Then it can be affirmed that the means compared are different due to
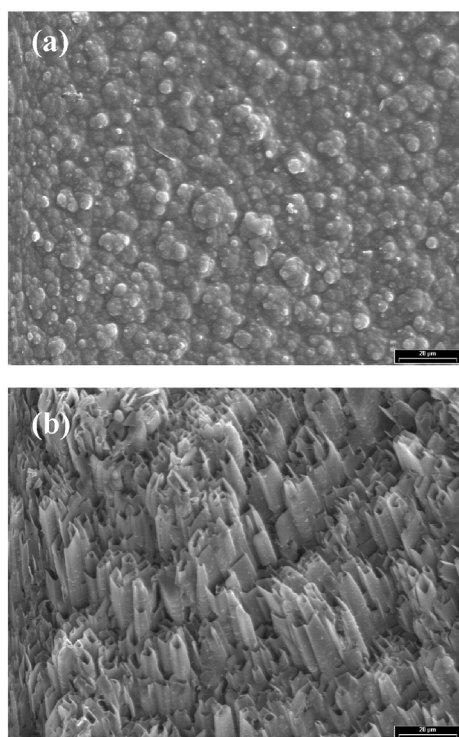
the different treatments and not due to experimental errors. The LSD test determined that the mean adherence force of all the samples were different, none of the means were similar to each other. So, the presence of NaSa in the electropolymerisation solution is significant in terms of adhesion of the samples.

3.2. Corrosion behaviour

One of the objectives of the present study was to examine the corrosion behaviour of the covered electrodes. The variation of OCP with time can be used as an indicator of the protection grade imparted by the polymer. This measure was taken for both coatings, $PPy_{0.1}$ and $PPy_{0.5}$, and then compared with the one obtained for bare NiTi (Fig. 2). A more positive potential is obtained for both coated electrodes, suggesting that the coatings provide anodic protection to NiTi.

The improved corrosion resistance can also be evaluated by comparing the polarisation curves in 0.15 M of chloride solution. The potentiodynamic run for bare NiTi (Fig. 3, curve a) shows a passive region followed by an increase in the current density at a mean value of 50 (2) mV (SCE), which indicates the breakdown of passivity. In the case of NiTi/$PPy_{0.1}$, the curve shows that oscillations appear at a mean potential value higher than 2000 (30) mV (SCE), denoting the onset of pitting corrosion (Fig. 3, curve b). On the contrary, for NiTi/$PPy_{0.5}$ the improvement in passivation is seen in the increase of the length of the passive region (Fig. 3, curve c).

In order to evaluate the pitting corrosion resistance of the covered electrodes, the current was measured when a constant potential of 0.65 V (SCE), which is above the pitting potential of the bare alloy, was applied. Current oscillations, that are a typical sign of pitting corrosion, were observed for the uncovered substrate (Fig. 4, curve a). A current increase was observed for NiTi/$PPy_{0.1}$ after 2 h of polarisation, which indicates that the presence of the film is not sufficient to keep chloride ions away from the surface of the alloy (Fig. 4, curve b). In contrast to these behaviours, the measured current for NiTi/$PPy_{0.5}$ is significantly smaller even after a considerable period of time (12 h) (Fig. 4, curve c).

Bare NiTi and the electrodes coated with $PPy_{0.5}$ and $PPy_{0.1}$ were examined after polarisation at 0.65 V (SCE) using SEM (Fig. 5). As was previously reported in our papers [10,11], the surface of bare NiTi alloy presents localised corrosion after applying this potential. The absence of any detectable change in the $PPy_{0.5}$ surface (Fig. 5a) indicates that pitting corrosion does not occur. In addition, the microtubes remain intact after the polarisation. On the contrary, the SEM image of the NiTi alloy covered with $PPy_{0.1}$ shows a completely deteriorated coating in
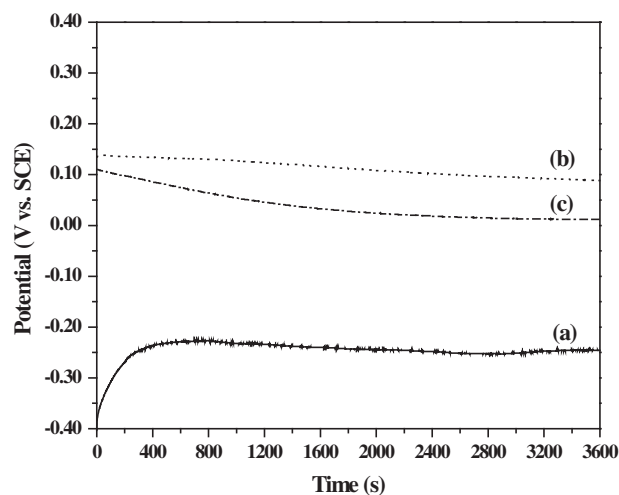

Fig. 1. SEM images of PPy electrosynthesised at 0.80 V (SCE) for 600 s in 0.25 M Py solution with: (a) 0.50 M NaSa and (b) 0.10 M NaSa.

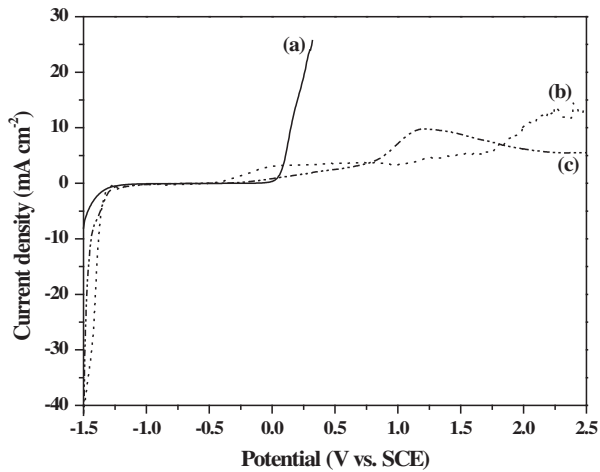**Fig. 2.** Time dependence of the OCP in 0.15 M of NaCl for: (a) NiTi, (b) NiTi/$PPy_{0.1}$ and (c) NiTi/$PPy_{0.5}$.

Fig. 3. Potentiodynamic polarisation curves of: (a) NiTi, (b) NiTi/PPy$_{0.1}$ and (c) NiTi/PPy$_{0.5}$ in 0.15 M of NaCl, scan rate 0.005 V s^{-1}.

several zones (Fig. 5b), indicating that localised corrosion occurs under the PPy film. The analysis of the amount of nickel and titanium released into the chloride solution are presented in Table 1. The data confirm that the dissolution of the alloy was significantly reduced by the presence of the PPy$_{0.5}$ coating.
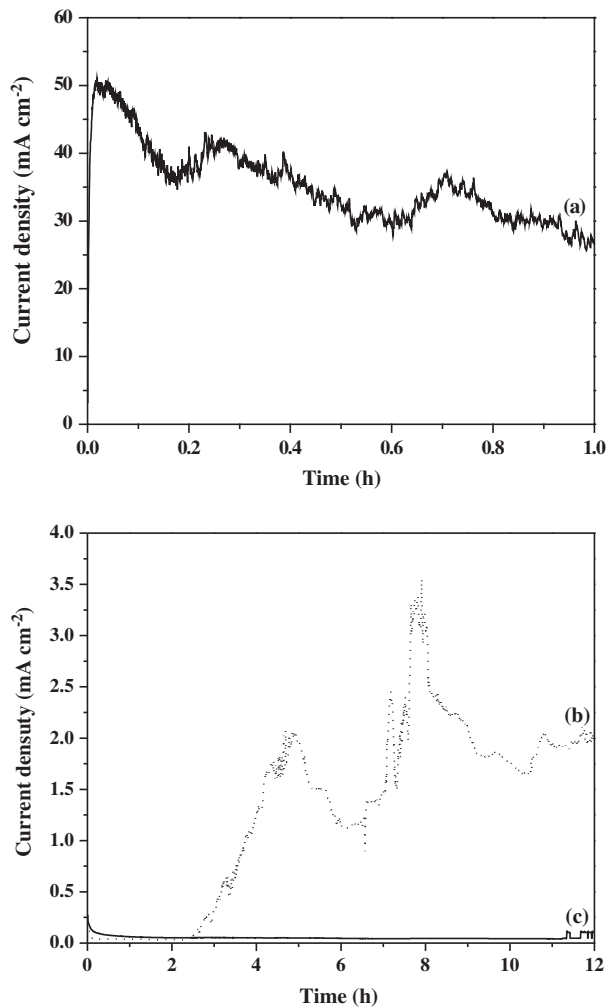

Fig. 4. Potentiostatic response obtained at 0.65 V in 0.15 M of NaCl solution for: (a) NiTi, (b) NiTi/PPy$_{0.1}$ and (c) NiTi/PPy$_{0.5}$.
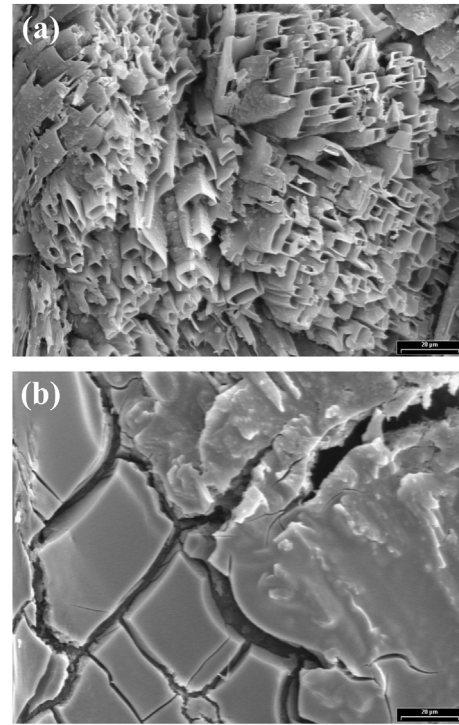

Fig. 5. SEM image obtained after polarisation at 0.65 V for 12 h in 0.15 M NaCl for: (a) NiTi/PPy$_{0.5}$ and (b) NiTi/PPy$_{0.1}$.

It is worth noticing that in a previous work, the same coatings, PPy$_{0.1}$ and PPy$_{0.5}$, were electrosynthesised onto 316L stainless steel and the best anticorrosion properties were provided by PPy$_{0.1}$ [34]. This was attributed to the porous opened structure of the microtubes. In order to determine the passivating effect of salicylate on both materials, polarisation curves for NiTi and 316L stainless steel were registered in 0.15 M of NaCl with and without NaSa (Fig. 6(A) and (B)). In the case of the polarisations of the bare alloys performed in 0.15 M of NaCl solution, both curves show a current increase at 0.25 V (SCE), denoting the beginning of pitting corrosion (Fig. 6(A) and (B) curves a). As it can be observed, the presence of NaSa produces a displacement in the pitting potential, reaching a more positive value in the case of NiTi. The results suggest that the improvement in the corrosion protection of PPy$_{0.5}$ when NiTi is used as substrate must be due to the higher amount of Sa available in the polymer matrix. Even though the structure of the microtubes is porous, the passivating effect of Sa prevails.

3.3. Silver deposition

The PPy electrosynthesised films are thought to be a propitious substrate to perform the deposition of a metal such as silver. The polymer can be used for the reduction of silver salts to metallic silver [12] and the oxidation degree of PPy is determinant in this process.

From the experiments detailed in Section 3.2 it can be concluded that the PPy$_{0.5}$ coating has better anticorrosion properties than PPy$_{0.1}$. Moreover, this coating has due to its morphology, a higher specific

Table 1
Concentration of Ni and Ti released after anodic polarisation in 0.15 M of NaCl solution for bare NiTi and the different PPy-coated NiTi alloy.

Sample	Applied potential (V (SCE))	Time (h)	Ni concentration (mg L^{-1})[a]	Ti concentration (mg L^{-1})[a]
Bare NiTi	0.65	0.5	14.96	4.41
NiTi/PPy$_{0.10}$	0.65	12	13.7	<0.05
NiTi/PPy$_{0.50}$	0.65	12	<0.05	<0.05

[a] In all cases, the standard deviation was <0.03.

area. Then deposition of silver was performed onto this covered electrode by immersion into a 0.05 M of $AgNO_3$ solution for 5 min under OCP conditions. After this, an anodic stripping sweep starting at 0.30 V (SCE) was recorded in 0.50 M of NaSa solution. The stripping response of the NiTi/$PPy_{0.5}$ electrode is presented in (Fig. 7, curve a). The onset of a peak at 0.31 V (SCE) is due to oxidation of the deposited Ag. The current increase at potentials higher than 0.70 V (SCE) is due to the oxidation of the polymer. In order to determine if the immersion time has an influence in the amount of silver deposited, the process was repeated for different immersion times. The results are also shown in Fig. 7, where it can be seen that the charge corresponding to Ag oxidation increases with the immersion time in the $AgNO_3$ solution (Fig. 7, curves b and c).

It was postulated that silver is deposited as a result of a redox reaction between the non-oxidised polymer segments and Ag^+ ions [18, 20]. Then, another objective of the present study is to evaluate the influence of a polymer pretreatment on the silver electrodeposition process. According to this, different potentials were applied to the PPy coated electrodes in a 0.50 M of NaSa solution in order to obtain different oxidation degrees of the polymer coating. After this, the electrodes were carefully rinsed with water, immersed in a 0.05 M of $AgNO_3$ solution and then an anodic stripping sweep was performed.

To choose the appropriate potentials to apply during the pretreatments, the voltammetric behaviour of a thinner $PPy_{0.5}$ film (formed at 0.80 V (SCE) during 80 s) was evaluated in a 0.50 M of NaSa solution.

Fig. 7. Anodic stripping in 0.50 M of NaSa ($E_i = 0.30$ V; $E_f = 1.00$ V, $v = 0.001$ V s^{-1}) for NiTi/$PPy_{0.50}$ after immersion in 0.05 M of $AgNO_3$ at OCP for: (a) 5 min; (b) 2 h and (c) 5 h.

The results are presented in Fig. 8. The potential was cycled repetitively between 0.60 V (SCE) and −1.20 V (SCE) at a scan rate of 0.05 V s^{-1}. The redox current peaks developed during cycling indicate that the deposited polymer is electrochemically active. The cathodic peak at −0.95 V (SCE) can be associated with cation (Na^+) transport which takes place to compensate the incomplete release of salicylate during PPy reduction [35].

According to the results presented in Fig. 8, to obtain a large amount of non-oxidised segments in the polymer, a potential of −1.00 V (SCE) was applied for 15 s. After the immersion in Ag^+ solution for only 5 min, a white deposit could be observed on the surface of the electrode. The experiment was repeated applying the same potential, but for 180 s. When the anodic sweeps were performed, it was observed that the peak charge corresponding to silver oxidation increases with the polarisation time (Fig. 9). The effect of this applied potential in the amount of deposited silver is very significant. For example, the stripping charge obtained for the untreated $PPy_{0.5}$ coating immersed for 5 h (Fig. 7, curve c) is smaller than the charge corresponding to the $PPy_{0.5}$ coating prepolarised at −1.00 V (SCE) for 180 s and then immersed in Ag^+ solution for only 5 min (Fig. 9, curve b).

A SEM analysis of the coatings confirmed the results of the anodic stripping curves. When the $PPy_{0.5}$ coating was not prepolarised, silver was deposited in the form of rosette-like aggregates (Fig. 10a). When
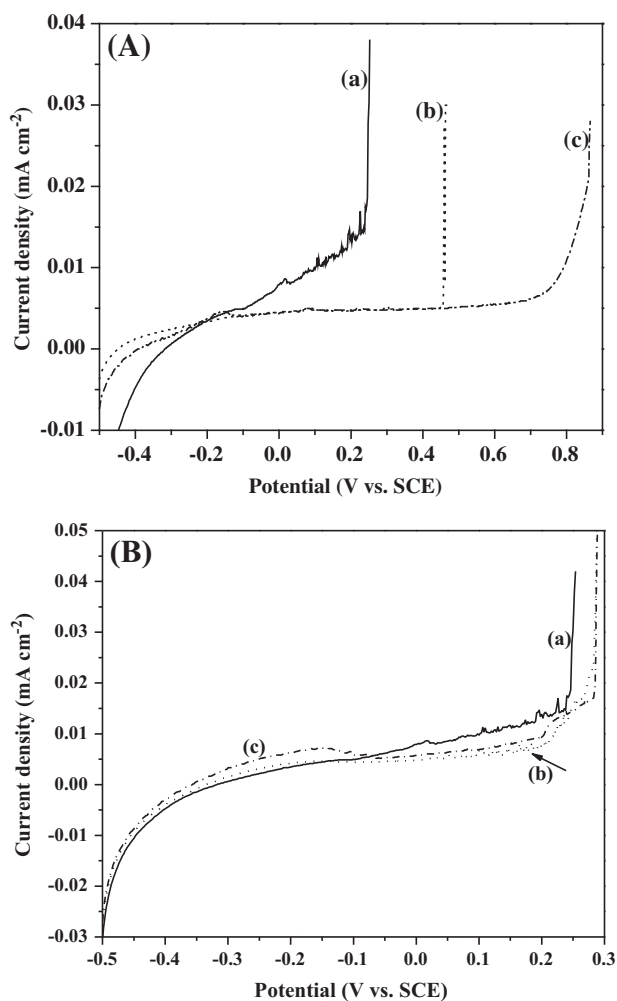

Fig. 6. Polarisation curves for (A) NiTi and (B) 316L stainless steel registered in (a) 0.15 M of NaCl solution (b) 0.15 M of NaCl + 0.01 M of NaSa and (c) 0.15 M of NaCl + 0.05 M of NaSa. In all the cases, the scan rate was 0.001 V s^{-1}.
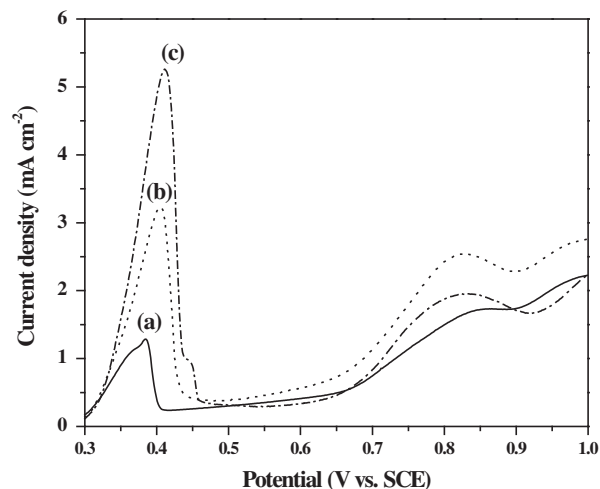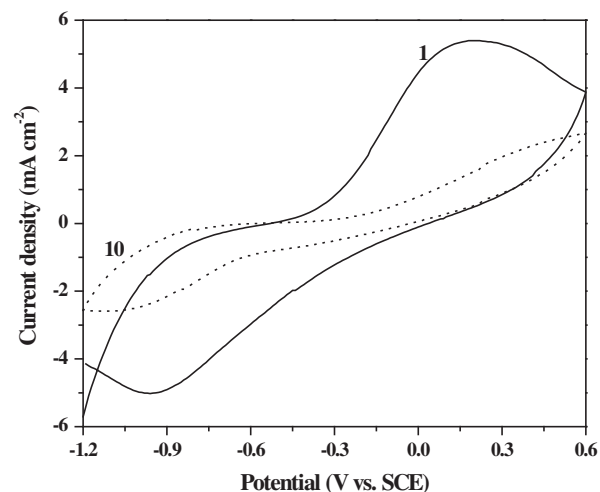

Fig. 8. Cyclic voltammograms obtained for NiTi/$PPy_{0.5}$ in 0.50 M of NaSa. The first (full line) and tenth (dotted line) cycles are displayed. Scan rate: 0.05 V s^{-1}. The films were formed potentiostatically at 0.80 V (SCE) for 80 s in 0.50 M of NaSa + 0.25 M of Py solution.
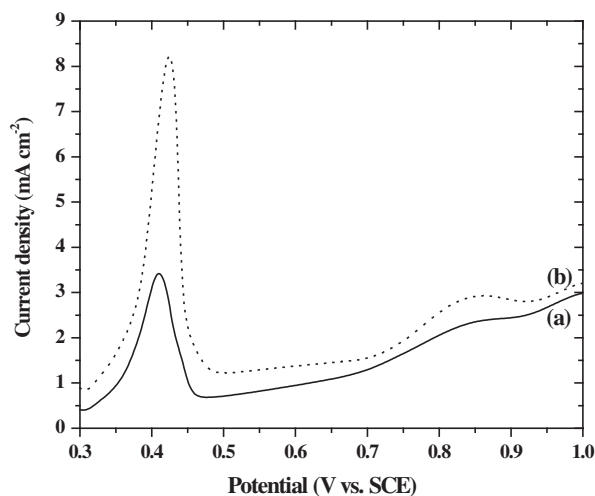
Fig. 9. Anodic stripping in 0.50 M of NaSa ($E_i = 0.30$ V; $E_f = 1.00$ V, $v = 0.001$ V s^{-1}) for NiTi/PPy$_{0.5}$prepolarised at -1.00 V (SCE) for (a) 15 s; (b) 180 s and then immersed in 0.05 M of AgNO$_3$ at OCP for 5 min.

the electrode was prepolarised at -1.00 V (SCE) the silver deposits were more uniform, covering completely the surface of the microtubes. In the case of the electrode prepolarised for 180 s (Fig. 10b) the amount of silver deposited is larger than the amount deposited after polarisation for 15 s (Fig. 10c). Under these conditions, the number of non-oxidised segments of the polymer increases and as a result the amount of deposited Ag is also increased. In all the cases, the presence of silver was checked through an EDX analysis (Fig. 10d).

The stripping results corresponding to a polarisation of -1.30 V (SCE) did not show a well-defined tendency with the variation of polarisation time. This behaviour might be explained considering that the pretreatment at this very negative potential might cause the loss of the polymer conductivity making the oxidation process difficult.

To obtain the response of the polymer with a high oxidation degree, the PPy-covered electrode was prepolarised at 0.80 V (SCE) before Ag deposition. In this case the stripping charges decrease with polarisation time and they are lower than those corresponding to the untreated electrode (Fig. 11, curves a and b).

The response of overoxidised polymer was also checked. The PPy-covered electrode was prepolarised at 1.20 V (SCE) during different times in a solution without the monomer. In this case, the stripping charges increase with the increment of polarisation time (Fig. 11, curves c and d). It is well known that overoxidation of conducting polymers causes a loss of electroactivity and conductivity. But on the other hand it was postulated that carbonyl and carboxyl groups are generated on the backbone of overoxidised PPy which promote cationic species to be accumulated onto the film [36,37]. Thus, the presence of these groups results in an enhancement of the silver ion concentration at the polymer surface.

The SEM analysis of the coatings again confirms the results obtained from the anodic stripping curves. In the case of the films prepolarised at 0.80 V (SCE), the amount of silver diminishes with the polarisation time (Fig. 12a and b), as a consequence of a decrease in the quantity of non-oxidised segments of the polymer. As a result, less Ag$^+$ ions can be reduced. It can be seen that the amount of silver for both polarisation pretreatments of 15 s is similar (Fig. 12 a and c). Likewise, polarisation at 0.80 V (SCE) for 180 s leads to an amount of silver almost imperceptible (Fig. 11 b). In the case of the PPy$_{0.5}$ coating prepolarised at 1.20 V (SCE) for 180 s, the quantity of silver was higher and the deposits formed have a needle shape (Fig. 12 d), a morphology previously reported [38].

To determine if the coatings maintain the good anticorrosion properties after the pretreatments and the immersion in AgNO$_3$ solution, the OCP was measured in 0.15 M of NaCl solution for one week (Fig. 13). It can be seen that for all the coatings the value of the OCP is more positive than the OCP value of the bare alloy. The amount of nickel and titanium released in the chloride solution was analysed and the values obtained are presented in Table 2. The results indicate that all the coatings can provide a good protection to the alloy for 7 days.
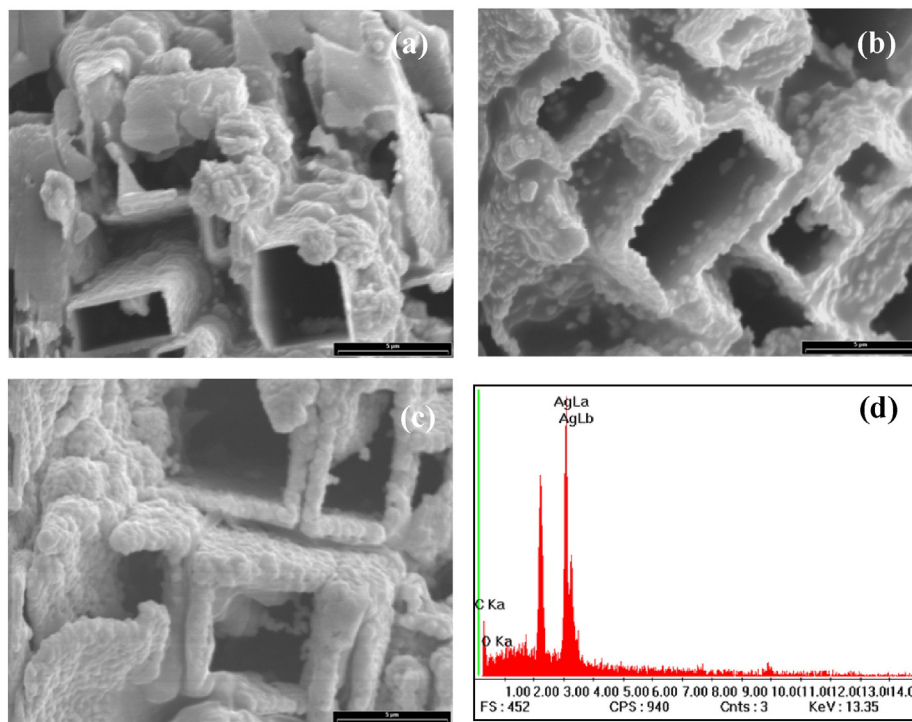

Fig. 10. SEM images for NiTi/PPy$_{0.50}$ (a) without polarisation and prepolarised at -1.00 V (SCE) for: (b) 15 s; (c) 180 s. After this the electrodes were immersed in 0.05 M of AgNO$_3$ at OCP for 5 min. (d) EDX analysis of the central area of (c).
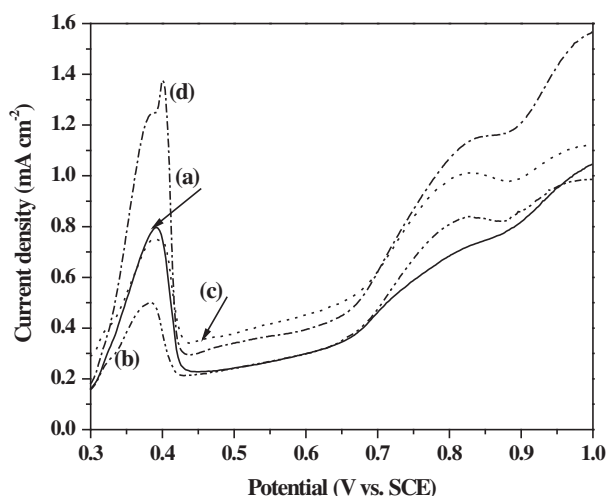
Fig. 11. Anodic stripping in 0.50 M of NaSa ($E_i = 0.30$ V; $E_f = 1.00$ V, $v = 0.001$ V s^{-1}) for NiTi/PPy$_{0.5}$prepolarised at (a) 0.80 V (SCE) for 15 s; (b) 0.80 V (SCE) for 180 s; (c) 1.20 V (SCE) for 15 s and (d) 1.20 V for 180 s. Then they were immersed in 0.05 M of AgNO$_3$ at OCP for 5 min.

Fig. 13. Time dependence of the OCP in 0.15 M of NaCl of the different PPy-coated NiTi alloys: (a) NiTi, (b) NiTi/PPy$_{0.5}$ (without silver), (c) NiTi/PPy$_{0.5}$, (d) NiTi/PPy$_{0.5}$ prepolarised at −1.00 V (SCE), (e) NiTi/PPy$_{0.5}$ prepolarised at 0.80 V (SCE), and (f) NiTi/PPy$_{0.5}$ prepolarised at 1.20 V (SCE). Then, for (c) to (f), the electrodes were immersed in a 0.05 M of AgNO$_3$ solution for 5 h.

3.4. Antibacterial activity

With the increase in healthcare-associated infections and the inability of conventional antimicrobial therapies to treat them, alternative methods of preventing staphylococcal biomaterial-related infections have gained much attention. Today, it is anticipated that an implant is colonised at the time of implantation due to the introduction of commensal skin bacteria, especially *S. aureus* (22–23.6%) and *S. epidermidis* (19–37.5%) [39].

Our results indicated that *S. aureus* ATCC 25923 was susceptible to all antibiotics tested, including the most common antimicrobials used in clinical therapy. In contrast, *S. epidermidis* was susceptible only
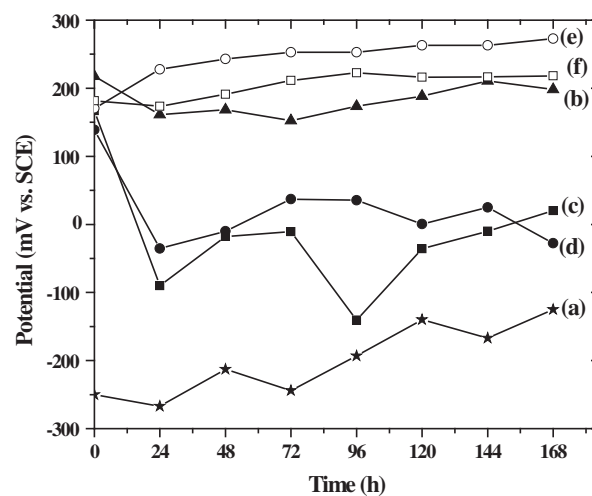
to vancomycin, tetracycline, chloramphenicol and nitrofurantoin. Therefore, it is considered as multiresistant.

Once established the resistance to antibiotics of these bacteria, we aimed to determine through an in vitro assay the antibacterial properties of NiTi/PPy$_{0.5}$/Ag compounds against the multidrug-resistant strain (*S. epidermidis*) and the drug-susceptible strain (*S. aureus* ATCC 25923).

Using the diameter of inhibition zone in disk diffusion test (Table 3) the antibacterial activity of NiTi/PPy$_{0.5}$/Ag compounds was compared to the strains. The diameter of the inhibition zone reflects the magnitude of susceptibility of the microorganism.

Because it has been shown that NiTi alloy [40] and salicylate themselves have antibacterial activity [41], bare NiTi and NiTi/PPy$_{0.5}$ were
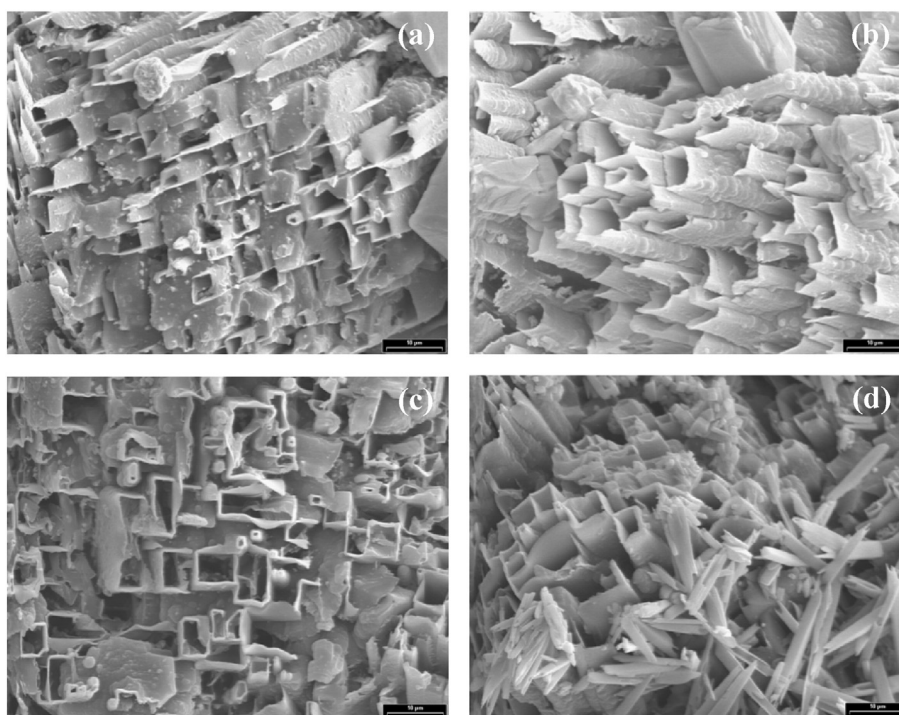

Fig. 12. SEM images for NiTi/PPy$_{0.50}$ (a) prepolarised at 0.80 V (SCE) for 15 s; (b) prepolarised at 0.80 V (SCE) for 180 s; (c) prepolarised at 1.20 V (SCE) for 15 s; (d) prepolarised at 1.20 V (SCE) for 180 s; then immersed in 0.05 M of AgNO$_3$ at OCP for 5 min.

Table 2
Concentration of Ni and Ti released after OCP in 0.15 M of NaCl solution for bare NiTi and the different PPy-coated NiTi alloys. For the prepolarised samples, the polarisation time was 180 s.

Sample	Applied potential (V (SCE))	Time of immersion in Ag$^+$ (h)	Ni concentration (mg L^{-1})[a]	Ti concentration (mg L^{-1})[a]
Bare NiTi	–	–	2.34	<0.05
NiTi/PPy$_{0.5}$	–	5	0.27	<0.05
NiTi/PPy$_{0.5}$	−1.00	5	<0.05	<0.05
NiTi/PPy$_{0.5}$	0.80	5	<0.05	<0.05
NiTi/PPy$_{0.5}$	1.20	5	<0.05	<0.05

[a] In all cases, the standard deviation was <0.03.

tested. Bare NiTi does not inhibit the antibacterial activity, but an inhibition zone of 2 mm was observed in the case of NiTi/PPy$_{0.5}$.

While both *S. aureus* and *S. epidermidis* depict a high sensitivity to the NiTi/PPy$_{0.5}$/Ag compounds, ATCC strain was more sensitive compared with the clinical strain. For *S. aureus* ATCC 25923, the size of the inhibition area was between 12 and 16 mm, with a clear demarcation between the edge of the area and the culture. It can be assessed that these species of *Staphylococcus* presented the highest sensitivity against the NiTi/PPy$_{0.5}$/Ag system showing the largest inhibition zones. For *S. epidermidis*, the zones of inhibition were in the 8–10 mm range. The *S. epidermidis* was less sensitive compared to the reference strain.

The fact that the drug-resistant and drug-susceptible strains were affected by NiTi/PPy$_{0.5}$/Ag compounds would indicate that the drug-resistant proteins that give bacteria the capacity to avoid antibiotics do not affect the efficacy of these compounds.

Antimicrobial mechanism of action of silver ions to microorganism cells is very complex. Several proposals have been developed to explain the antimicrobial effects of silver ions. First, silver ions bind to the cell envelope, thereby causing a change in their structure and permeability and inactivation proteins [42,43]. Finally, the silver ions penetrate into the cell and inhibit various proteins in the cytoplasm and ribosome and interact with nucleic acids preventing replication and translation processes, causing cell death [44,45].

The data presented here illustrates the potential biocidal effect of NiTi/PPy$_{0.5}$/Ag compounds to different microbial strains, including highly multiresistant bacteria such as *S. epidermidis* used in this work. Certainly, the use of clinical strains isolated from patients with infection provides the antimicrobial activity of NiTi/PPy/Ag compounds in current medical practice.

Regardless of the immersion time employed (2 min versus 5 h), the diameter of the inhibition zone did not differ in any of the tested bacteria. Since the inhibition zone was measured on agar plates using a ruler with 1 mm resolution, the possibility of measurement errors exists. These results indicate that the inhibitory activity of the coated electrodes is independent of the immersion time during the coating preparation.

The statistical analysis was performed for each strain. The values of F and p were 264.0 and 0.0001 in the case of the *S. aureus* and 99.67 and 0.0003 for *S. epidermidis*. In both cases, the LSD test demonstrated that

mean values of the samples covered with Ag did not differ from one another.

4. Conclusions

Polypyrrole films could be electrosynthesised onto NiTi alloy in the presence of NaSa. The morphology of the films depended on the NaSa concentration: granular morphology for low concentrations and hollow rectangular microtubes for high concentrations. The OCP measurements in NaCl suggest that both coatings provide anodic protection to the alloy, but the PPy$_{0.1}$ was not able to protect the substrate from the pitting corrosion process.

The silver deposition process can be carried out at OCP conditions. The amount of silver deposited depended on the immersion time in AgNO$_3$ solution and the oxidation degree of the polymer. The maximum amount of silver was obtained when the PPy$_{0.5}$ was prepolarised at −1.00 V (SCE) for 180 s in NaSa solution. This result suggests that a great quantity of non-oxidised segments is obtained by polarising the polymer with a negative potential. All the PPy$_{0.5}$/Ag coatings can still provide corrosion protection to the alloy after one week of immersion in NaCl solution at OCP conditions.

The antibacterial test against *S. aureus* and *S. epidermidis* for NiTi/PPy$_{0.5}$ electrodes prepolarised at −1.00 V (SCE) for 180 s and then immersed in AgNO$_3$ demonstrated that they have a good antibacterial activity.

References

[1] M.T. Andani, N.S. Moghaddam, C. Haberland, D. Dean, M.J. Miller, M. Elahinia, Metals for bone implants. Part 1. Powder metallurgy and implant rendering, Acta Biomater. 10 (2014) 4058–4070.
[2] T. Duerig, A. Pelton, D. Stöckel, An overview of nitinol medical applications, Mater. Sci. Eng. A 273–275 (1999) 149–160.
[3] X. Liu, P.K. Chu, C. Ding, Surface modification of titanium, titanium alloys, and related materials for biomedical applications, Mater. Sci. Eng. R 47 (2004) 49–121.
[4] A.R. Oller, M. Costa, G. Oberdorster, Carcinogenicity assessment of selected nickel compounds, Toxicol. Appl. Pharmacol. 66 (1997) 143–152.
[5] Y.P. Kathuria, The potential of biocompatible metallic stents and preventing restenosis, Mater. Sci. Eng. A 417 (2006) 40–48.
[6] N.K. Guimard, N. Gomez, C.E. Schmidt, Conducting polymers in biomedical engineering, Prog. Polym. Sci. 32 (2007) 876–921.
[7] M.B. González, S.B. Saidman, Electrodeposition of polypyrrole on 316L stainless steel for corrosion prevention, Corros. Sci. 53 (2011) 276–282.
[8] I.L. Lehr, S.B. Saidman, Characterisation and corrosion protection properties of polypyrrole electropolymerised onto aluminium in the presence of molybdate and nitrate, Electrochim. Acta 51 (2006) 3249–3255.
[9] U. Rammelt, L.M. Duc, W. Plieth, Improvement of protection performance of polypyrrole by dopant anions, J. Appl. Electrochem. 35 (2005) 1225–1230.
[10] D.O. Flamini, S.B. Saidman, Electrodeposition of polypyrrole onto NiTi and the corrosion behaviour of the coated alloy, Corros. Sci. 52 (2010) 229–234.
[11] D.O. Flamini, M. Saugo, S.B. Saidman, Electrodeposition of polypyrrole on Nitinol alloy in the presence of inhibitor ions for corrosion protection, Corros. Sci. 81 (2014) 36–44.
[12] J. Stejskal, Conducting polymer–silver composites, Chem. Pap. 67 (2013) 814–848.
[13] K. FirozBabu, P. Dhandapani, S. Maruthamuthu, M. Anbu Kulandainathan, One pot synthesis of polypyrrole silver nanocomposite on cotton fabrics for multifunctional property, Carbohydr. Polym. 90 (2012) 1557–1563.
[14] Y. Peng, L. Qiu, C. Pan, C. Wang, S. Shang, F. Yan, Facile preparation of water dispersible polypyrrole nanotube-supported silver nanoparticles for hydrogen peroxide reduction and surface-enhanced Raman scattering, Electrochim. Acta 75 (2012) 399–405.
[15] X. Yang, L. Li, F. Yan, Polypyrrole/silver composite nanotubes for gas sensors, Sensors Actuators B 145 (2010) 495–500.
[16] N.L. Pickup, J.S. Shapiro, D.K.Y. Wong, Extraction of silver by polypyrrole films upon a base–acid treatment, Anal. Chim. Acta 364 (1998) 41–51.

Table 3
Inhibition zone diameter for the different NiTi/PPy$_{0.5}$ coatings.[a]

Sample	Applied potential (V (SCE))	Time of immersion in Ag$^+$ (h)	Diameter of the inhibition zones (mm)	
			S. aureus ATCC 25923	*S. epidermidis*
NiTi	–	–	0	0
NiTi/PPy$_{0.50}$	–	–	2 (0)	2 (0)
NiTi/PPy$_{0.50}$	−1.00	5 h	15 (0)	10 (0)
NiTi/PPy$_{0.50}$	−1.00	2 min	14 (2)	9 (1)

[a] Mean values, with sample standard deviations in parentheses.

[17] A.A. Arrieta Almario, R.L. Vieira, Study of polypyrrole films modified with copper and silver microparticles by electrochemical cementation process, J. Chil. Chem. Soc. 3 (2006) 971–974.

[18] M.B. González, L.I. Brugnoni, M.E. Vela, S.B. Saidman, Silver deposition on polypyrrole films electrosynthesized in salicylate solutions, Electrochim. Acta 102 (2013) 66–71.

[19] E. Pintér, R. Patakfalvi, T. Fülei, Z. Gingl, I. Dékány, C. Visy, Characterization of polypyrrole — silver nanocomposites prepared in the presence of different dopants, J. Phys. Chem. B 109 (2005) 17474–17478.

[20] F.Y. Song, K.K. Shiu, Preconcentration and electroanalysis of silver species at polypyrrole film modified glassy carbon electrodes, J. Electroanal. Chem. 498 (2001) 161–170.

[21] M.B. González, S.B. Saidman, Electrosynthesis of hollow polypyrrole microtubes with a rectangular cross-section, Electrochem. Commun. 13 (2011) 513–516.

[22] M.B. González, O.V. Quinzani, M.E. Vela, A.A. Rubert, G. Benítez, S.B. Saidman, Study of the electrosynthesis of hollow rectangular microtubes of polypyrrole, Synth. Met. 162 (2012) 1133–1139.

[23] P.J.G. Goulet, R.F. Aroca, Chemical adsorption of salicylate on silver — a systematic approach to the interpretation of surface-enhanced vibrational spectra, Can. J. Chem. 82 (2004) 987–997.

[24] M.C. Alvarez-Ros, S. Sánchez-Cortés, J.V. García-Ramos, Vibrational study of the salicylate interaction with metallic ions and surfaces, Spectrochim. Acta A 56 (2000) 2471–2477.

[25] C. von Eiff, B. Jansen, W. Kohner, K. Becker, Infections associated with medical devices: pathogenesis, management and prophylaxis, Drugs 65 (2005) 179–214.

[26] P. Stoodley, G.D. Ehrlich, P.P. Sedghizadeh, L. Hall-Stoodley, M.E. Baratz, D.T. Altman, N.G. Sotereanos, J.W. Costerton, P. DeMeo, Orthopaedic biofilm infections, Curr. Orthop. Pract. 22 (2011) 558–563.

[27] B. Thornes, P. Murray, D. Bouchier-Hayes, Development of resistant strains of Staphylococcus epidermidis on gentamicin-loaded bone cement in vivo, J. Bone Joint Surg. (Br.) 84 (2002) 758–760.

[28] D. Campoccia, L. Montanaro, P. Speziale, C.R. Arciola, Antibiotic-loaded bio-materials and the risks for the spread of antibiotic resistance following their prophylactic and therapeutic clinical use, Biomaterials 31 (2010) 6363–6377.

[29] A. Dion, M. Langman, G. Hall, M. Filiaggi, Vancomycin release behaviour from amorphous calcium polyphosphate matrices intended for osteomyelitis treatment, Biomaterials 26 (2005) 7276–7285.

[30] N. Rameshbabu, T.S.S. Kumar, T.G. Prabhakar, V.S. Sastry, K.V.G.K. Murty, K.P. Rao, Antibacterial nanosized silver substituted hydroxyapatite: synthesis and characterization, J. Biomed. Mater. Res. 80A (2007) 581–591.

[31] R.G. Carrodeguas, S. De Aza, Tricalcium phosphate: synthesis, properties and biomedical applications, Acta Biomater. 7 (2011) 3536–3546.

[32] A.W. Bauer, M.M. Kirby, J.C. Sherris, M. Tuurck, Antibiotic susceptibility testing by a standardized single disk method, Am. J. Clin. Pathol. 45 (1966) 493–496.

[33] Clinical and Laboratory Standards Institute, Performance standards for antimicrobial susceptibility testing, 15th Informational Supplement, CLSI Document M100-S15, Wayne, USA, 2005.

[34] M.B. González, S.B. Saidman, Corrosion protection properties of polypyrrole electropolymerized onto steel in the presence of salicylate, Prog. Org. Coat. 75 (2012) 178–183.

[35] A.C. Cascalheira, S. Aeiyach, P.C. Lacaze, L.M. Abrantes, Electrochemical synthesis and redox behaviour of polypyrrole coatings on copper in salicylate aqueous solution, Electrochim. Acta 48 (2003) 2523–2529.

[36] J. Li, X. Lin, Electrodeposition of gold nanoclusters on overoxidized polypyrrole film modified glassy carbon electrode and its application for the simultaneous determination of epinephrine and uric acid under coexistence of ascorbic acid, Anal. Chim. Acta 596 (2007) 222–230.

[37] M. Sahin, Y. Sahin, A. Ozcan, Ion chromatography-potentiometric detection of inorganic anions and cations using polypyrrole and overoxidized polypyrrole electrode, Sensors Actuators B 133 (2008) 5–14.

[38] S. Chang, K. Chen, Q. Hua, Y. Ma, W. Huang, Evidence for the growth mechanisms of silver nanocubes and nanowires, J. Phys. Chem. C 115 (2011) 3513–3527.

[39] J.R. Lentino, Prosthetic joint infections: bane of orthopedists, challenge for infectious disease specialists, Clin. Infect. Dis. 36 (2003) 1157–1161.

[40] P. Li, X. Zhang, R. Xu, W. Wang, X. Liu, K.W. Yeung, P.K. Chu, Electrochemically deposited chitosan/Ag complex coatings on biomedical NiTi alloy for antibacterial application, Surf. Coat. Technol. 232 (2013) 370–375.

[41] R.E. Polonio, L.A. Mermel, G.E. Paquette, J.F. Sperry, Eradication of biofilm forming Staphylococcus epidermidis (RP62A) by a combination of sodium salicylate and vancomycin, Antimicrob. Agents Chemother. 45 (2001) 3262–3266.

[42] A.D. Russell, W.B. Hugo, Antimicrobial activity and action of silver, Prog. Med. Chem. 31 (1994) 351–370.

[43] W.K. Jung, H.C. Koo, K.W. Kim, S. Shin, S.H. Kim, Y.H. Park, Antibacterial activity and mechanism of action of the silver ion in Staphylococcus aureus and Escherichia coli, Appl. Environ. Microbiol. 74 (2008) 2171–2178.

[44] H.J. Klasen, A historical review of the use of silver in the treatment of burns. II. Renewed interest for silver, Burns 26 (2000) 131–138.

[45] Q.L. Feng, J. Wu, G.Q. Chen, F.Z. Cui, T.N. Kim, J.O. Kim, A mechanistic study of the antibacterial effect of silver ions on Escherichia coli and Staphylococcus aureus, J. Biomed. Mater. Res. 52 (2000) 662–668.